

Bridging the mass gaps at $A = 5$ and $A = 8$ in nucleosynthesis*

H. Oberhummer^a, A. Cs  t  b^b, and H. Schlattl^c

^aInstitute of Nuclear Physics, Vienna University of Technology,
Wiedner Hauptstra  e 8-10, A-1040 Vienna, Austria

^bDepartment of Atomic Physics, E  tv  s University,
P  zm  ny P  ter s  t  ny 1/A, H-1117 Budapest, Hungary

^cMax-Planck-Institut f  r Astrophysik,
Karl-Schwarzschild-Stra  e 1, D-85741 Garching, Germany

In nucleosynthesis three possible paths are known to bridge the mass gaps at $A = 5$ and $A = 8$. The primary path producing the bulk of the carbon in our Universe proceeds via the triple-alpha process ${}^4\text{He}(2\alpha, \gamma){}^{12}\text{C}$. This process takes place in helium-burning of red giant stars. We show that outside a narrow window of about 0.5 % of the strength or range of the strong force, the stellar production of carbon or oxygen through the triple-alpha process is reduced by factors of 30 to 1000. Outside this small window the creation of carbon or oxygen and therefore also carbon-based life in the universe is strongly disfavored. The anthropically allowed strengths of the strong force also give severe constraints for the sum of the light quark masses as well as the Higgs vacuum expectation value and mass parameter at the 1 % level.

1. INTRODUCTION

Few-body methods are used in nuclear astrophysics for the determination of thermonuclear cross sections and reaction rates predominantly for nuclei with mass numbers up to about $A = 12$. These reactions are of relevance for primordial nucleosynthesis, i.e., the production of nuclei up to $A = 7$ in standard Big-Bang model. In the inhomogeneous Big-Bang nucleosynthesis model nuclei with $A > 7$ can also be produced. Few-body methods play also a role in the determination of reaction rates for the pp-chains in main-sequence stars up to $A = 7$ and helium burning from $A = 4$ to $A = 12$. Finally, in the alpha-rich freeze-out occurring in supernovae, reaction rates for nuclei from $A = 4$ to $A = 12$ are studied using few-body methods.

We want to discuss the bridging of the mass gaps at $A = 5$ and $A = 8$ in nucleosynthesis through three-body reactions (Fig. 1). The following paths via three-body reactions can bridge these mass gaps:

*This work was partly supported by the Fonds zur wissenschaftlichen Forschung in   sterreich (P13246-TPH), D32513/FKFP-0242-2000/BO-00520-98 (Hungary) and by the John Templeton Foundation (938-COS153). We would like to thank A. Weiss for useful discussions, and B. Gr  n, S. Haslinger and T. Strodl for their assistance in preparing this paper.

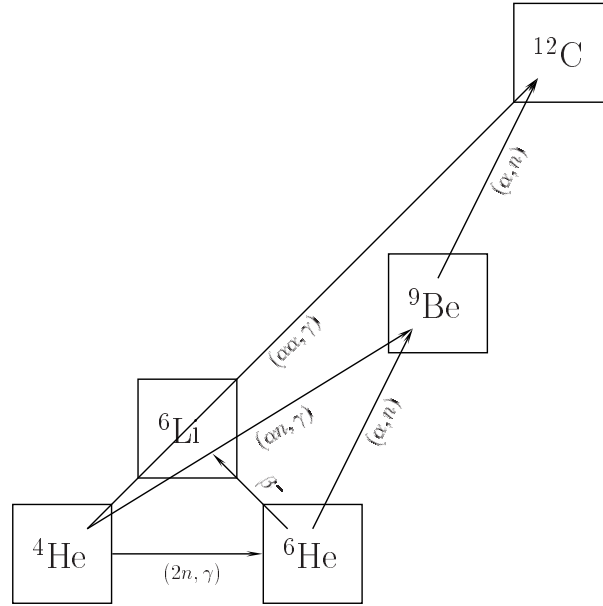


Figure 1. Possible reaction paths bridging the mass numbers $A = 5$ and $A = 8$.

1. Reaction path ${}^4\text{He}(2n, \gamma){}^6\text{He}(\alpha, n){}^9\text{Be}(\alpha, n){}^{12}\text{C}$: Under representative conditions the reaction path ${}^4\text{He}(2n, \gamma){}^6\text{He}(\alpha, n){}^9\text{Be}(\alpha, n){}^{12}\text{C}$ can be neglected in known astrophysical scenarios, because the fragile ${}^6\text{He}$ is destroyed very effectively by photodissociation ${}^6\text{He}(\gamma, 2n){}^4\text{He}$ [1–3]. The cross sections and reaction rates for the reaction ${}^4\text{He}(2n, \gamma){}^6\text{He}$ and the reverse photodissociation have been calculated using an $\alpha+n+n$ approach [2].
2. Reaction path ${}^4\text{He}(\alpha n, \gamma){}^9\text{Be}(\alpha, n){}^{12}\text{C}$: This reaction path is dominant in the so-called alpha-rich freeze-out occurring in type II supernovae [1,4–7]. The cross sections and the reaction rates for ${}^4\text{He}(\alpha n, \gamma){}^9\text{Be}$ and the reverse photodissociation have been calculated in a semimicroscopic model and compared with the experimental data [7].
3. Triple-alpha process ${}^4\text{He}(2\alpha, \gamma){}^{12}\text{C}$: The bulk of the carbon in the universe is produced through this process in the helium-burning phase of red giant stars. The reaction rate for the triple-alpha process has been determined recently in a microscopic 12-nucleon model [8–10].

In the following section we will present the calculation of the reaction rate for the triple-alpha process in the microscopic 12-nucleon model ${}^4\text{He}(2\alpha, \gamma){}^{12}\text{C}$. Sect. 3 will be devoted to variations of the nucleon-nucleon (N-N) force and its consequences for the stellar production of carbon and oxygen in the universe. In Sect. 4 we discuss the constraints for anthropically allowed parameters of elementary particle physics like the light quark masses or the Higgs vacuum expectation value and mass parameter. In the last section a short summary is given.

2. REACTION RATE FOR THE TRIPLE-ALPHA PROCESS

The formation of ^{12}C in hydrogen burning is blocked by the absence of stable elements at mass numbers $A = 5$ and $A = 8$. Öpik [11] and Salpeter [12] pointed out that the lifetime of ^8Be is long enough, so that the $\alpha + \alpha \rightleftharpoons ^8\text{Be}$ reaction can produce macroscopic amounts of equilibrium ^8Be in stars. Then, the unstable ^8Be could capture an additional α particle to produce stable ^{12}C . However, this so-called triple-alpha reaction has very low rate since the density of ^8Be in the stellar plasma is very low, because of its short lifetime of 10^{-16} s.

Hoyle (cited in [13]) argued that the triple-alpha reaction cannot produce enough carbon in a non-resonant way in order to explain the measured abundance in the Universe, therefore it must proceed through a hypothetical resonance of ^{12}C , thus strongly enhancing the cross section. Hoyle suggested that this resonance is a $J^\pi = 0^+$ state at about $\varepsilon = 0.4$ MeV (throughout this paper ε denotes resonance energy in the center-of-mass frame relative to the three-alpha threshold, while Γ denotes the full width). Subsequent experiments indeed found a 0^+ resonance in ^{12}C in the predicted energy region by studies of the reaction $^{14}\text{N}(d,\alpha)^{12}\text{C}$ [13,14] and the β^- -decay of ^{12}B [15]. It is the second 0^+ state (0_2^+) in ^{12}C . Its modern parameters, $\varepsilon = 0.3796$ MeV and $\Gamma = 8.5 \times 10^{-6}$ MeV [16], agree well with the old theoretical prediction.

2.1. Microscopic 12-body model

The astrophysical models that determine the amount of carbon and oxygen produced in red giant stars need some nuclear properties of ^{12}C as input parameters. Namely, the position and width of the 0_2^+ resonance, which almost solely determines the triple-alpha reaction rate, and the radiative decay width for the $0_2^+ \rightarrow 2_1^+$ transition in ^{12}C . We calculated these quantities in a microscopic 12-body model [8–10].

In the microscopic cluster model it is assumed that the wave functions of certain nuclei, like ^{12}C , contain, with large weight, components which describe the given nucleus as a compound of 2-3 clusters. By assuming rather simple structures for the cluster internal states, the relative motions between the clusters, which are the most important degrees of freedom, can be treated rigorously. The strong binding of the free alpha particle ^4He makes it natural that the low-lying states of ^{12}C have 3α -structures [17]. Therefore, our cluster-model wave function for ^{12}C looks like

$$\Psi^{12\text{C}} = \sum_{l_1, l_2} \mathcal{A} \left\{ \Phi^\alpha \Phi^\alpha \Phi^\alpha \chi_{[l_1 l_2] L}^{\alpha(\alpha\alpha)}(\boldsymbol{\rho}_1, \boldsymbol{\rho}_2) \right\}. \quad (1)$$

Here \mathcal{A} is the intercluster antisymmetrizer, the Φ^α cluster internal states are translationally invariant $0s$ harmonic-oscillator shell-model states with zero total spin, the $\boldsymbol{\rho}$ vectors are the intercluster Jacobi coordinates, l_1 and l_2 are the angular momenta of the two relative motions, L is the total orbital angular momentum and $[\dots]$ denotes angular momentum coupling. The total spin and parity of ^{12}C are $J = L$ and $\pi = (-1)^{l_1+l_2}$, respectively.

We performed calculations using the Minnesota (MN) and modified Hasegawa-Nagagata (MHN) N-N forces. These two forces give the best simultaneous description of the ^8Be ground state and the 0_2^+ state of ^{12}C [10], in agreement with the experience gained in the cluster-model description of the structure and reactions of various light nuclei [18]. The

MN-force is given by [19,20]

$$V_{ij}(r) = \left(V_1(r) + \frac{1}{2}(1 + P_{ij}^\sigma)V_2(r) + \frac{1}{2}(1 - P_{ij}^\sigma)V_3(r) \right) \left(\frac{1}{2}u + \frac{1}{2}(2 - u)P_{ij}^r \right) + V_{ij}^{\text{Coul.}}(r), \quad (2)$$

where P^r and P^σ are the space- and spin-exchange operators, respectively, u is the exchange mixture parameter, $r = |\mathbf{r}_j - \mathbf{r}_i|$, and $V_{ij}^{\text{Coul.}}$ is the Coulomb force between the two nucleons. The MHN force is given by [21]

$$V_{ij}(r) = \sum_{k=1}^3 \left(W_k + M_k P_{ij}^r + B_k P_{ij}^\sigma + H_k P_{ij}^\tau \right) V_k(r) + V_{ij}^{\text{Coul.}}(r). \quad (3)$$

The parameter W_k is the Wigner parameter, P_{ij}^r , P_{ij}^σ , and P_{ij}^τ are the space-, spin-, and isospin-exchange operators (Majorana-, Bartlett-, and Heisenberg-operators), and M_k , B_k , and H_k are the corresponding exchange mixture parameters.

The spatial parts of the MN- and MHN-force have Gaussian forms

$$V_k(r) = V_{0k} \exp \left[- \left(\frac{r}{r_{0k}} \right)^2 \right], \quad k = 1, 2, 3, \quad (4)$$

where V_{0k} and r_{0k} are the strength and range parameters of the potentials, respectively.

2.2. Triple-alpha reaction rate

The resonant reaction rate for the triple-alpha process proceeding via the ground state of ^8Be and the 0_2^+ resonance in ^{12}C is given approximately by [22]

$$r_{3\alpha} \approx 3^{\frac{3}{2}} N_\alpha^3 \left(\frac{2\pi\hbar^2}{M_\alpha k_B T} \right)^3 \frac{\Gamma_\gamma}{\hbar} \exp \left(- \frac{\varepsilon}{k_B T} \right), \quad (5)$$

where M_α and N_α are the mass and the number density of the alpha particle, while \hbar and k are Planck's and Boltzmann's constant, respectively. The temperature of the stellar plasma is given by T .

We calculated the resonance energy ε of the 0_2^+ state in ^{12}C , relative to the 3α -threshold, and the $0_2^+ \rightarrow 2_1^+$ radiative (E2) width Γ_γ . The 0_2^+ state is situated above the 3α -threshold, therefore for a rigorous description one has to use an approach which can describe three-body resonances correctly. We choose the complex scaling method [23] that has already been used in a variety of other nuclear physics problems, see e.g. [17,24,25].

As a first step of our calculations, we fine tune each N-N force (by slightly changing their exchange-mixture parameters) to fix ε in Eq. (5) at its experimental value. The other important quantity that needs to be calculated is the radiative width of the 0_2^+ state, coming from the electric dipole (E2) decay into the 2_1^+ state of ^{12}C . This calculation involves the evaluation of the E2 operator between the initial 0_2^+ three-body scattering state and the final 2_1^+ bound state [26]. The proper three-body scattering-state treatment of the 0_2^+ initial state is not feasible in our approach for the time being, therefore we use a bound-state approximation to it. This is an excellent approximation for the calculation of Γ_γ because the total width of the 0_2^+ state is very small (8.5 eV [16]). The value of Γ_γ is rather sensitive to the energy difference between the 0_2^+ and 2_1^+ states, so we have to make sure that the experimental energy difference is correctly reproduced.

2.3. Stellar-model calculations

The composition of the interstellar material (ISM) is a mixture of ejecta from stars with different masses. At present it is not clear which type of stars contribute most of the ^{12}C or ^{16}O to the ISM. Therefore, we performed stellar model calculations for a typical massive, intermediate-mass and low-mass star with masses 20 , 5 , and $1.3 M_{\odot}$, respectively, including the calculated triple-alpha reaction rates.

We used a modern stellar evolution code, which contains the most recent input physics [27]. Up-to-date solar models can be calculated with this program [28] as well as the evolution of low-mass stars can be followed through the thermal-pulse phase of stars at the asymptotic giant branch [29]. The nuclear network is designed preferentially to calculate the H- and He-burning phases in low-mass stars. Additionally, all basic reactions of C- and O-burning are included, which may destroy the previously produced C and O in massive and intermediate-mass stars.

Here, the stars are followed from the onset of H-burning until the third thermal pulse on the AGB, or until the core temperature reaches 10^9 K in the case of the $20 M_{\odot}$ star (the nuclear network is not sufficient to go beyond this phase).

Large portions of the initial mass of a star are returned to the ISM through stellar winds. Unfortunately, basically due to the simple convection model used in stellar modeling, the composition of the wind cannot yet be determined very accurately from stellar evolution theory. However, it is beyond the scope of the present investigations to determine how and when the material is returned to the ISM. Instead we examine how much C and O is produced altogether.

For the $1.3 M_{\odot}$ star, which loses its envelope basically during the thermal-pulse phase, the maximum C and O abundances in the He-burning region have been extracted. Although the efficiency of the dredge-up of heavy elements to the surface is only badly known, it is independent of the nuclear physics, and hence should be similar in all models independent of the triple-alpha rate. By taking the maximum abundances in this region, we have a measure of how strongly the enrichment of the stellar envelope by C or O is altered by modifying the triple-alpha rate.

In the 5 and $20 M_{\odot}$ stars further fusion reactions like C- and O-burning take place. The dredge-up process of metal-enriched material under these circumstances is more complicated and more uncertain than in the $1.3 M_{\odot}$ star. The $20 M_{\odot}$ star finally even explodes in a supernova. Therefore, for the 5 and $20 M_{\odot}$ stars the total amount of C and O in the stellar interior is evaluated.

3. VARIATIONS OF THE NUCLEON-NUCLEON FORCE

In this section we slightly vary the strength and range parameters of the MN- and MHN-potentials and calculate the modified resonance energies ε and gamma widths Γ_{γ} of the 0_2^+ state in ^{12}C . With these values of ε and Γ_{γ} we recalculate the triple-alpha reaction rate $r_{3\alpha}$ of Eq. (5). We find that the value of Γ_{γ} is very little changed by the small variations of the N-N interactions, leading to negligible changes in $r_{3\alpha}$. Thus, in the stellar model calculations we can fix Γ_{γ} to its experimental value in all cases. The resonance energy ε , however, is rather sensitive to variations in the N-N force, leading to large changes in the triple-alpha rate $r_{3\alpha}$. By making the N-N force weaker, the resonance

energy ε moves higher and the reaction rate $r_{3\alpha}$ decreases exponentially as can be seen from Eq. (5). The opposite is true for a stronger N-N force.

We have done a series of tests in order to make sure that the main assumptions of our calculations remain valid while the interactions are varied. Here we mention only three main points. We checked that the use of Eq. (5) is justified for all the different resonance energies as well as temperatures occurring in our calculations. In all cases the triple-alpha reaction is dominated by the sequential process through the ${}^8\text{Be}$ ground state and the 0_2^+ state of ${}^{12}\text{C}$. The amount of variations in the strength of the Coulomb and strong interaction are small enough to keep the experimental ${}^8\text{Be}$ ground state and the 0_2^+ state of ${}^{12}\text{C}$ from becoming a broad state or a bound state. We also estimated the non-resonant contribution [30], without the 0_2^+ resonance in ${}^{12}\text{C}$, to the triple-alpha rate and found that this contribution is about 7-13 orders of magnitude smaller than the resonant contribution in the stellar temperature range $T \approx (0.8 - 3) \times 10^8$ K arising in our stellar-model calculations. Furthermore, the contribution of the next higher-energy 0^+ resonance (at about 2.7 MeV above the three-alpha threshold [22]) to the triple-alpha rate is smaller by about 40 orders of magnitude in the considered temperature range. Also, in the above temperature range the reaction will not proceed through the low-energy wing of the ${}^8\text{Be}$ resonance [30].

Some of the carbon, produced in the triple-alpha process, is further synthesized in the ${}^{12}\text{C}(\alpha, \gamma){}^{16}\text{O}$ and ${}^{16}\text{O}(\alpha, \gamma){}^{20}\text{Ne}$ reactions. The ${}^{16}\text{O}(\alpha, \gamma){}^{20}\text{Ne}$ reaction is nonresonant, so variations in the strengths of the strong force can have only small effects on its reaction rate. The ${}^{12}\text{C}(\alpha, \gamma){}^{16}\text{O}$ process may look more dangerous because its cross section is strongly affected by subthreshold states in the ${}^{16}\text{O}$ nucleus [22]. However, if the N-N force is made weaker, then the subthreshold states become less bound, thereby enhancing the ${}^{12}\text{C}(\alpha, \gamma){}^{16}\text{O}$ cross section. Therefore, in the case of a weaker force the small C/O ratio is further decreased. An analogous reasoning holds for a stronger force. Thus, without doing any calculation for the ${}^{12}\text{C}(\alpha, \gamma){}^{16}\text{O}$ and ${}^{16}\text{O}(\alpha, \gamma){}^{20}\text{Ne}$ reactions with the modified forces, we can conclude that their effect would strengthen our hypothesis regarding carbon and oxygen production.

There may be other windows for different values of the fundamental interactions in which an appreciable amount of carbon and oxygen could be produced. The window that seems to be closest to the values realized in our universe is the creation of oxygen and carbon in the big bang [31]. This possibility is prevented in our universe by the existence of the stability gaps at mass numbers $A = 5$ and $A = 8$. In order to make ${}^5\text{He}$ or ${}^5\text{Li}$ as well as ${}^8\text{Be}$ become bound, we calculated that the strong forces would have to be increased by about 10%, a value that is about a factor 20 larger than the maximal variation investigated in this work.

We multiply now in the MN- and MHN-potentials independently the strength parameters V_{0k} as well as the range parameters r_{0k} for all repulsive and attractive terms V_{0k} in Eq. (4) by the same factor p . This factor was set between 0.994 and 1.006 for the strength parameters and 0.997 and 1.003 for the range parameters of the MN and MHN potentials. With these values for the factor p we recalculate the resonance energies and the triple-alpha reaction rates. For each of these new reaction rates we then perform again the corresponding stellar model calculations.

The resulting changes in the C and O abundances are shown (Fig. 2) with respect to

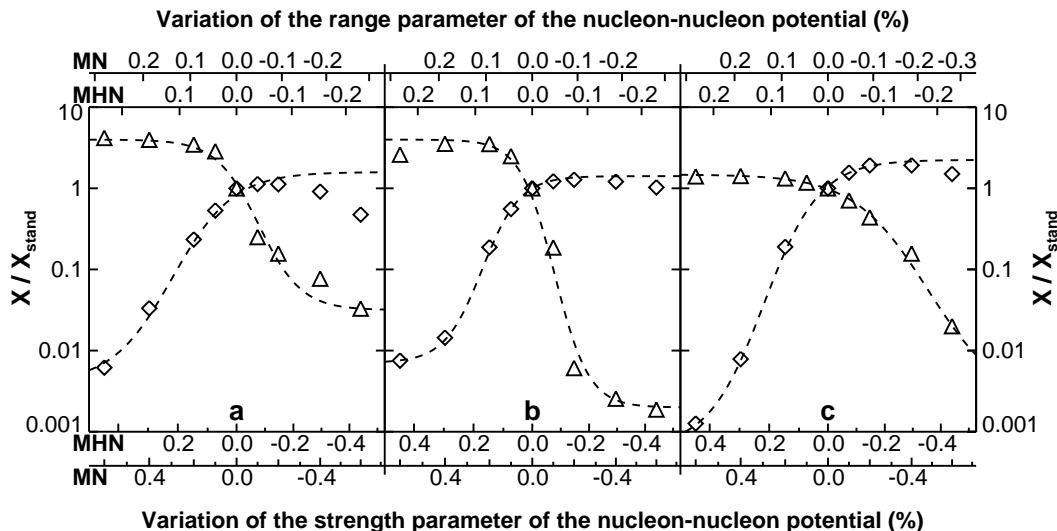


Figure 2. The change of the carbon (Δ) and oxygen (\diamond) mass abundances (X) through variations of the strength (lower ordinate) and range parameters (upper ordinate) of the nucleon-nucleon potentials MN and MHN. The abundance changes are shown in panels a, b, and c for stars with masses of 20, 5, and $1.3 M_{\odot}$, respectively, in units of the standard values X_{stand} . The dashed curves are drawn to guide the eye.

the case, where the standard value of the resonance energy has been used (i.e., with no variations of the strength or range parameters of the MN- and MHN-potentials). Because each shift in the resonance energy can be identified with a variation in the strength or range parameter of the corresponding N-N force, we scaled the lower and upper ordinate with variations in these quantities, respectively.

We conclude that a change of more than about 0.5% in the strength parameters or 0.2-0.3% in the range parameters of the MHN- or MN-potential would destroy either nearly all C or all O in every star. This implies that irrespective of stellar evolution the contribution of each star to the abundance of C or O in the ISM would be negligible. This corresponds to a fine tuning that is about two orders of magnitude better than obtained from the constraints of a bound deuteron [32–34] or from the non-existence of a bound diproton or dineutron [35].

In Fig. 2 one can see that the size of the resulting change in the abundances with the variation of the range parameters r_{0k} is about twice the size of the change coming from the variation of the strength parameters V_{0k} . This can be understood quite simply, because we only considered small variations ($\approx 0.5\%$) of the strength and range parameters, respectively. In this case the changes in the strength and range parameters in Eq. (4)

$$\begin{aligned} V'_{0k} &= (1 \pm \delta V_{0k})V_{0k}, \\ r'_{0k} &= (1 \pm \delta r_{0k})r_{0k} \end{aligned} \tag{6}$$

lead to a change in the spatial parts in the potential for $\delta r_{0k} \ll 1$

$$\begin{aligned} V'_k(r) &= V'_{0k} \exp \left[- \left(\frac{r}{r_{0k}} \right)^2 \right] = (1 \pm \delta V_{0k}) V_k(r), \\ V'_k(r) &= V_{0k} \exp \left[- \left(\frac{r}{r'_{0k}} \right)^2 \right] \approx V_{0k} \exp \left[- (1 \mp 2\delta r_{0k}) \left(\frac{r}{r_{0k}} \right)^2 \right] \approx (1 \pm 2\delta r_{0k}) V_k(r), \end{aligned} \quad (7)$$

where in the second line we used a mean potential range parameter $r \approx r_{0k}$ in the first-order correction term. Therefore, in the above approximation a change in the range parameter r_{0k} corresponds to a twice as large change, $\delta V_{0k} \approx +2\delta r_{0k}$, in the strength parameter.

4. ANTHROPOLOGICALLY ALLOWED QUARK MASSES AND HIGGS PARAMETERS

In this section we investigate the constraints on the anthropically allowed quark masses following largely the discussion already given in Ref. [36].

The one-boson exchange potential (OBEP) for the N-N force can be written as a sum of Yukawa terms

$$V_{\text{OBEP}}(r) = -f_\pi^2 \frac{\exp(-m_\pi r)}{r} - f_\sigma^2 \frac{\exp(-m_\sigma r)}{r} + f_\omega^2 \frac{\exp(-m_\omega r)}{r}, \quad (8)$$

where the f 's and m 's are the coupling constants and masses of the π , σ and ω mesons, respectively. The OBEP-potential has a long-range tail from one-pion exchange, an attractive minimum due to the exchange of the hypothetical σ -meson and a repulsive core due to the ω -meson. In the following we will only consider the long-range part due to the pion, the one-pion exchange potential (OPEP),

$$V_{\text{OPEP}}(r) = -f_\pi^2 \frac{\exp(-m_\pi r)}{r}. \quad (9)$$

For small changes of the pion mass,

$$m'_\pi = m_\pi \pm \delta m_\pi, \quad (10)$$

we obtain

$$V'_{\text{OPEP}}(r) = -f_\pi^2 \frac{\exp(-m'_\pi r)}{r} \approx -f_\pi^2 \frac{\exp[-(m_\pi \pm \delta m_\pi)r]}{r} \approx \left(1 \mp \frac{\delta m_\pi}{m_\pi} \right) V_{\text{OPEP}}(r), \quad (11)$$

where in the second line we used a mean potential range given by the pion mass $r \approx 1/m_\pi$ in the first-order correction term.

The range defined by the inverse pion-mass is therefore also limited to a $\pm 0.5\%$ window. Here we assumed that the sensitivity of the carbon production to the potential strength is similar in the OPEP and MN/MHN cases, respectively.

As long as the up- and down-quark masses are small compared to the QCD scale, the mass of the pion is well approximated by $m_\pi \propto \sqrt{f_\pi(m_u + m_d)}$ [33,34]. Therefore, the sum of the up- and down-quark masses $m_{u+d} \equiv m_u + m_d$ scales with the pion mass

m_π as $0.5\delta m_{u+d} \approx \delta m_\pi$. Thus the anthropically allowed value of the sum of the up- and down-quark masses are fine tuned to approximately 1%. Using the quark masses $m_u = (4.88 \pm 0.57)$ MeV and $m_d = (9.81 \pm 0.65)$ MeV the anthropically allowed sum of the up- and down-quark masses m_{u+d} is constrained to within about 0.15 MeV. This is consistent with the result of Ref. [36] where a value in the order of 0.05 MeV is given.

Constraints can also be obtained for the difference of the down- and up-quark masses, $m_{d-u} \equiv m_d - m_u$. We do not consider possible variations of the electron mass as in Ref. [36]. The constraint for the upper limit of δm_{d-u} follows from the restriction that the pp-fusion



is exothermic. This gives an allowed range of $\delta m_{d-u} < 0.42$ MeV. The constraint for the lower limit of δm_{d-u} follows from the stability of the hydrogen atom, i.e. that the proton capture of an electron



is endothermic. This gives an allowed range of $\delta m_{d-u} > -0.782$ MeV. The stability of the proton and deuteron give also constraints for the lower and upper limit of δm_{d-u} . However, these constraints are less stringent than the ones obtained from the ones given above [36].

The resulting anthropically allowed strengths of the up- and down-quark masses are given by the central region of Fig. 3. As can be seen from this figure the anthropic fine tuning of the up- and down-quark masses is less than a few percent. The band around $\delta m_d/m_d = -0.5\delta m_u/m_u$ determined by the production of carbon and oxygen is about four times narrower than the band around $\delta m_d/m_d = +0.5\delta m_u/m_u$. That means that the constraints of carbon or oxygen production give a stronger fine tuning than the constraints determined from the reactions of Eqs. (12) and (13). If additional joint constraints that unification imposes on the fermion masses like the ratio m_d/m_e are taken into account [37], three-dimensional constraining plots for the up-quark, down-quark and electron masses can be derived.

Similar considerations [33,34,38] can be carried out for the Higgs vacuum expectation value $v \approx \sqrt{-\mu^2/\lambda} \propto \mu$ and the Higgs mass parameter μ . Since the up- and down-quark masses scale simply with the Higgs vacuum expectation value, the Higgs vacuum expectation value v and Higgs mass parameter μ are also fine tuned by anthropic considerations to approximately $\pm 1\%$.

5. SUMMARY

In this work we have shown that the strength or range of the strong force is fine tuned to $\pm 0.5\%$ by the production of carbon or oxygen and therefore also carbon-based life. This leads to a fine tuning of the sum of the light quark masses as well as the Higgs vacuum expectation value and mass parameter to about $\pm 1\%$.

One of the most fascinating aspects resulting from this is that life, stars, nuclei and elementary particles seem to be closely interwoven in our universe through this extreme fine tuning. It is not clear if the values of the fundamental parameters corresponding to

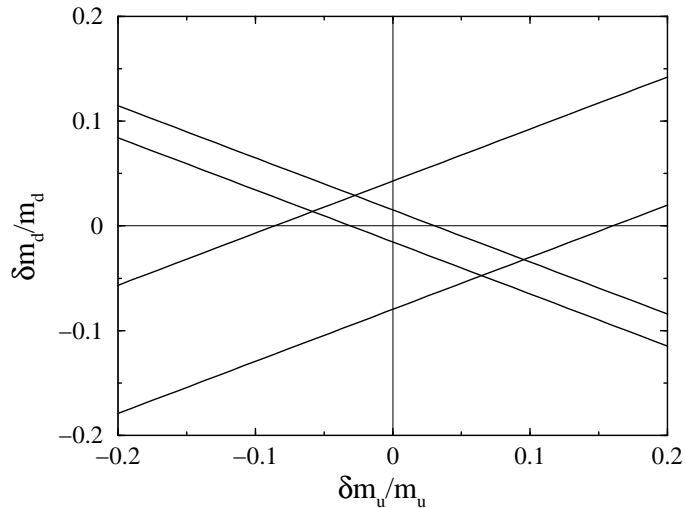


Figure 3. The central region shows the anthropically allowed values of variations of the up-quark mass $\delta m_u/m_u$ and variations of the down-quark mass $\delta m_d/m_d$. The following constraints are determined by the straight lines in the figure: (i) the pp-fusion in Eq. (12) is exothermic, (ii) the proton capture of an electron in Eq. (13) is endothermic, (iii) the carbon production is not suppressed, and (iv) the oxygen is production is not suppressed. These four constraints determine the upper and lower bounds of the bands around $\delta m_d/m_d = +0.5\delta m_u/m_u$ and $\delta m_d/m_d = -0.5\delta m_u/m_u$, respectively.

this anthropic fine tuning will be calculable by a future Final Theory [39] or if some of the parameters of such a Final Theory will have to be chosen from a large or continuous ensemble [36]. In any case it will be one of the challenges for a possible Final Theory to explain the anthropic fine tuning as described in this paper.

REFERENCES

1. J. Görres, H. Herndl, I.J. Thompson, and M. Wiescher, Phys. Rev. C 52 (1995) 2231.
2. V.D. Efros, W. Balogh, H. Herndl, R. Hofinger, and H. Oberhummer, Z. Phys. A 355 (1996) 101.
3. H. Herndl, R. Hofinger, and H. Oberhummer, Proceedings of the Origin of Matter and Evolution of Galaxies (OMEG97), Atami, Japan, S. Kubono, T. Kajino, K.I. Nomoto, and I. Tanihata (eds.), World Scientific, 1999, p. 233.
4. S.E. Woosely, J.R. Wilson, G.J. Mathews, R.D. Hoffmann, and B.S. Meyer, Astrophys. J. 433 (1994) 229.
5. K. Takahashi, J. Wittl, and H.T. Janka, Astron. and Astrophys. 286 (1994) 857.
6. S.E. Woosely and R.D. Hoffman, Astrophys. J. 395 (1992) 202.
7. V.D. Efros, H. Oberhummer, A.V. Pushkin, and I.J. Thompson, Europ. Phys. Jour. A 1 (1998) 447.
8. H. Oberhummer, A. Csótó, and H. Schlattl, Science 289 (2000) 88.
9. H. Oberhummer, A. Csótó, and H. Schlattl, Proceedings of the Symposium "The

- Future of the Universe and the Future of our Civilization”, Budapest-Debrecen, 2-6 July 1999, V. Burdyuzha and G. Khozin (eds.), World Scientific, Singapore, 2000, p. 197.
10. A. Csótó, H. Oberhummer, and H. Schlattl, Proceedings of the International Symposium on Exotic Nuclear Structures, Debrecen, Hungary, May 15-20, 2000, in press.
 11. G.K. Öpik, Proc. Roy. Irish Acad. A54 (1951) 49.
 12. E.E. Salpeter, Phys. Rev. 88 (1952) 547.
 13. D.N.F. Dunbar, R.E. Pixley, W.A. Wenzel, and W. Whaling, Phys. Rev. 92 (1953) 649.
 14. F. Hoyle, D.N.F. Dunbar, W.A. Wenzel, and W. Whaling, Phys. Rev. 92 (1953) 1095.
 15. C.W. Cook, W.A. Fowler, and T. Lauritsen, Phys. Rev. 107 (1957) 508.
 16. F. Ajzenberg-Selove, Nucl. Phys. A 490 (1988) 1.
 17. R. Pichler, H. Oberhummer, A. Csótó, and S.A. Moszkowski, Nucl. Phys. A 618 (1997) 55.
 18. K. Langanke, Adv. Nucl. Phys. 21 (1994) 85.
 19. I. Reichstein and Y.C. Tang, Nucl. Phys. A 158 (1970) 529.
 20. D.R. Thompson, M. LeMere, and Y.C. Tang, Nucl. Phys. A 286 (1977) 53.
 21. H. Furutani *et al.*, Prog. Theor. Phys. Suppl. 68 (1980) 193.
 22. C.E. Rolfs and W.S. Rodney, Cauldrons in the Cosmos, Univ. of Chicago Press, Chicago, 1988.
 23. Y.K. Ho, Phys. Rep. 99 (1983) 1.
 24. A.T. Kruppa, R.G. Lovas, and B. Gyarmati, Phys. Rev. C 37 (1988) 383.
 25. A. Csótó, Phys. Rev. C 49 (1994) 3035.
 26. P.J. Brussaard and P.W.M. Glaudemans, Shell-model applications in nuclear spectroscopy, North-Holland Publishing, Amsterdam 1977.
 27. A. Weiss and H. Schlattl, Astron. Astrophys. Suppl. 144 (2000) 487.
 28. H. Schlattl and A. Weiss, Astron. Astrophys. 347 (1999) 272.
 29. J. Wagenhuber and A. Weiss, Astron. Astrophys. 286 (1994) 121.
 30. K. Langanke, M. Wiescher, and F.-K. Thielemann, Z. Phys. A 324 (1986) 147.
 31. R.A. Alpher, H.A. Bethe, and G. Gamow, Phys. Rev. 73 (1948) 803.
 32. T. Pochet, J.M. Pearson, G. Beaudet, and H. Reeves, Astron. Astrophys. 143 (1991) 1.
 33. V. Agrawal, S.M. Barr, J.F. Donoghue, and D. Seckel, Phys. Rev. Lett. 80 (1998) 1822.
 34. V. Agrawal, S.M. Barr, J.F. Donoghue, and D. Seckel, Phys. Rev. D 57 (1998) 5480.
 35. F.J. Dyson, Scientific American 225 (1971) 51.
 36. C.J. Hogan, submitted to Reviews of Modern Physics Colloquia, Pre-print available at <http://xxx.lanl.gov/abs/astro-ph/9909295>.
 37. M. Fukugita, M. Tanimoto, and T. Yanagida, Phys. Rev. D 59 (1999) 113016.
 38. T.S. Jeltema and M. Sher, Phys. Rev. D 61 (2000) 017301.
 39. G.L. Kane, M.J. Perry, and A.N. Zytlow, Pre-print available at <http://xxx.lanl.gov/abs/astro-ph/0001197>.